Hybrid phase-space simulation method for interacting Bose fields

Scott E. Hoffmann, Joel F. Corney, and Peter D. Drummond

ARC Centre for Quantum-Atom Optics, School of Physical Sciences, University of Queensland, Brisbane, Queensland 4072, Australia

We introduce an approximate phase-space technique to simulate the quantum dynamics of interacting bosons. With the future goal of treating Bose-Einstein condensate systems, the method is designed for systems with a natural separation into highly occupied (condensed) modes and lightly occupied modes. The method self-consistently uses the Wigner representation to treat highly occupied modes and the positive-*P* representation for lightly occupied modes. In this method, truncation of higher-derivative terms from the Fokker-Planck equation is usually necessary. However, at least in the cases investigated here, the resulting systematic error, over a finite time, vanishes in the limit of large Wigner occupation numbers. We tested the method on a system of two interacting anharmonic oscillators, with high and low occupations, respectively. The hybrid method successfully predicted atomic quadratures to a useful simulation time 60 times longer than that of the positive-*P* method. The truncated Wigner method also performed well in this test. For the prediction of the correlation in a quantum nondemolition measurement scheme, for this same system, the hybrid method gave excellent agreement with the exact result, while the truncated Wigner method showed a large systematic error.

I. INTRODUCTION

The aim of this paper is to introduce a new, approximate, stochastic phase-space method and to test it on some simple problems with interacting Bose fields. A future goal of our research is to use the method to simulate the dynamics of interacting Bose-Einstein condensates (BECs). The method is, in fact, designed for BEC problems, since it relies on the ability to make a meaningful separation of a multimode system into highly occupied (condensed) modes and lightly occupied modes. Hence, our two-mode test cases will be constructed to have one highly occupied mode ($N \gg 1$) and one lightly occupied mode ($N \lesssim 1$).

Previous authors have developed formalisms in which condensed atoms are treated in a different way to noncondensed atoms. Castin and Dum [1] studied the dynamics of Bose-Einstein condensates at very low temperatures using a Bogoliubov [2] approach, in which the boson field operator is written as a sum of condensate-mode terms and noncondensate-mode terms. Their treatment deals with number eigenstates rather than coherent states. They obtain results as an asymptotic expansion in the square root of the fraction of noncondensed atoms. Gardiner and Zoller [3], in the third of their series on quantum kinetic theory, consider a stationary noncondensate band at a fixed temperature acting as a reservoir to the dynamic condensate modes. They derive a master equation for the condensate modes, using a number-conserving formalism. Dalton [4] calculates quantum correlation functions for boson field operators to use in the interpretation of double-well BEC interferometry experiments. The approach is a phase-space method for a distribution functional, in which the Wigner representation is used for the condensed modes and the positive-*P* representation for the noncondensed modes. Our method will be seen to be substantially different from these three approaches.

Besides in BEC evolution and collision problems, other typical cases where disparate occupation numbers exist would be in the quantum Brownian motion of a small number of massive particles inside a BEC, or in the collision of weak and strong coherent light pulses in a nonlinear optical fiber. Hence, we also consider these systems to be candidates for the hybrid method.

The foundations of this work are the stochastic phase-space methods developed to simulate the quantum dynamics of systems with many degrees of freedom. In particular we consider the Wigner-Moyal [5,6] approach, and the positive-*P* method [7,8]. We will see that both methods have wide applicability, but are ultimately limited in the parameter regimes on which they can be used. The Wigner-Moyal method generally requires a truncation to be able to map to a stochastic process. The resulting approximate theory typically fails to give correct results when significant numbers of modes with small mode occupation numbers are present [9].

The positive-*P* method is exact, but when applied to large multimode problems can often be used only for limited simulation times before very large sampling error renders it unusable. The longest useful simulation times, for a given interaction strength, are for lightly occupied modes [7].

The phase-space method to be introduced here is a combination of the Wigner and positive-*P* methods. In this hybrid method, as we will call it, highly occupied modes are treated with the Wigner representation while lightly occupied modes use the positive-*P* representation. A truncation of higher-order derivative terms is usually needed, but the resulting approximate method is expected to be valid (over finite times) to within corrections of the order of the reciprocal of the large occupation numbers.

The Wigner method is used in the regime where it is known to perform best and produces most simplification of the stochastic differential equations. The positive-*P* method is used on the modes that introduce the most errors in the truncated Wigner method. This latter choice is also designed to lengthen the useful simulation time.

In this paper we will summarize the properties of the two representations, and discuss their successes and problems, before actual construction of the hybrid method. As a test case, we will apply the method to an exactly solvable prob-

lem: A system of two coupled anharmonic oscillators, one highly occupied, the other lightly occupied. The interaction preserves individual particle numbers.

At first we simply calculate the expectation values of quadratures and compare with the truncated Wigner method, the positive-P method, and the exact solution. Then we investigate a higher-order correlation in the same system, one that would be observed in a quantum nondemolition measurement (QND) scheme.

II. SINGLE AND DOUBLED WIGNER REPRESENTATIONS

We consider a quantum many-body system of bosons. The relevant creation and annihilation operators are denoted $\hat{a}_m^\dagger$, $\hat{a}_m$. In the Wigner-Moyal approach, one complex phase-space variable, α_m, is used for each mode, m, of a system, and we call this a single phase space. In contrast, a doubled phase space uses two complex variables, α_m and α_m^+, for each mode. We will find that using the Wigner and positive-P representations for different modes of the same system will generally require using a doubled phase space, although this can be avoided in certain cases.

We begin by showing the definition and properties of the doubled Wigner representation. This is an extension of the familiar single phase-space Wigner representation to a doubled phase space, and has been studied and applied by Plimak *et al.* [10]. Throughout this paper we will set $\hbar = 1$.

The single phase-space Wigner representation of the density matrix is given by

$$\hat{\rho} = \int d^2\alpha \, W(\alpha) \hat{\Lambda}_W(\alpha). \tag{2.1}$$

This is an expansion of the density matrix on a basis of operators, the standard form we will use to compare all representations. Here $W(\alpha)$ is the Wigner function on phase space. Following Moyal [6] and Glauber and Cahill [11],

$$\hat{\Lambda}_W(\alpha) = \int \frac{d^2\xi}{\pi} e^{(\xi\hat{a}^\dagger - \xi^*\hat{a})} e^{(\alpha\xi^* - \alpha^*\xi)} \tag{2.2}$$

is an operator function on phase space, with trace unity. We also refer to this as the operator basis. We note that Eq. (2.1) has a unique inverse, defining the Wigner function in terms of the density matrix,

$$W(\alpha) = \int \frac{d^2\xi}{\pi^2} e^{(-\xi\alpha^* + \xi^*\alpha)} \text{Tr}(\hat{\rho} e^{(\xi\hat{a}^\dagger - \xi^*\hat{a})}). \tag{2.3}$$

By manipulating Eq. (2.2), these basis operators can be written in the normally ordered Gaussian form of Corney and Drummond [12],

$$\hat{\Lambda}_W(\alpha) = 2{:}e^{-2(\hat{a}^\dagger - \alpha^*)(\hat{a}-\alpha)}{:}, \tag{2.4}$$

where $:f(\hat{a}, \hat{a}^\dagger):$ indicates normal ordering.

Now we may define the doubled Wigner representation with an expansion of the density matrix of the form

$$\hat{\rho} = \int d^2\alpha \int d^2\alpha^+ \mathcal{W}(\alpha, \alpha^+) \hat{\Lambda}_{\mathcal{W}}(\alpha, \alpha^+). \tag{2.5}$$

Here $\mathcal{W}(\alpha, \alpha^+)$ is a Wigner function defined on a doubled phase space and

$$\hat{\Lambda}_{\mathcal{W}}(\alpha, \alpha^+) = 2{:}e^{-2(\hat{a}^\dagger - \alpha^+)(\hat{a}-\alpha)}{:} \tag{2.6}$$

are the operator basis elements, also defined on the doubled phase space. The new variable α^+ appears where α^* had been, but in a stochastic simulation may take values different from the complex conjugate of α.

From Eq. (2.6) we can derive the operator correspondences for the doubled Wigner representation. The action of a creation or annihilation operator, multiplying the density matrix to the left-hand or right-hand sides, is equivalent to a linear differential operator acting on the Wigner function,

$$\hat{a}\hat{\rho} \leftrightarrow \left(\alpha + \frac{1}{2}\frac{\partial}{\partial\alpha^+}\right)\mathcal{W}(\alpha, \alpha^+), \tag{2.7}$$

$$\hat{\rho}\hat{a} \leftrightarrow \left(\alpha - \frac{1}{2}\frac{\partial}{\partial\alpha^+}\right)\mathcal{W}(\alpha, \alpha^+), \tag{2.8}$$

$$\hat{a}^\dagger\hat{\rho} \leftrightarrow \left(\alpha^+ - \frac{1}{2}\frac{\partial}{\partial\alpha}\right)\mathcal{W}(\alpha, \alpha^+), \tag{2.9}$$

$$\hat{\rho}\hat{a}^\dagger \leftrightarrow \left(\alpha^+ + \frac{1}{2}\frac{\partial}{\partial\alpha}\right)\mathcal{W}(\alpha, \alpha^+). \tag{2.10}$$

We add a cautionary note. The derivation of Eqs. (2.7)–(2.10) depends on the vanishing of boundary terms in an integration by parts. This problem is discussed in Sec. IV.

We note that a pure coherent state (with $\rho = |\gamma\rangle\langle\gamma|$) can be represented, in the doubled Wigner representation, with the stochastic prescription

$$\alpha = \gamma + \frac{1}{2}(n_1 + in_2), \tag{2.11}$$

$$\alpha^+ = \gamma^* + \frac{1}{2}(n_1 - in_2), \tag{2.12}$$

where n_1 and n_2 are independent real Gaussian random noises with unit standard deviations.

In this symmetrically ordered representation, the formula for estimating symmetrically averaged products of creation and annihilation operators as stochastic averages over trajectories is

$$\langle \hat{a}^{\dagger m}\hat{a}^n \rangle_{\text{sym}} = \langle\langle \alpha^{+m}\alpha^n \rangle\rangle. \tag{2.13}$$

We will use the notation $\langle\langle\cdots\rangle\rangle$ throughout to signify a stochastic average over an ensemble of trajectories.

We note that we will be exploiting the nonuniqueness of this representation and that of the positive-P representation: An infinity of different functions $\mathcal{W}(\alpha, \alpha^+)$ can give the same density matrix according to Eq. (2.5). This feature of representations on doubled phase spaces will allow us, in the case of the hybrid representation, to construct quasiprobabilities

that are everywhere real and non-negative, obeying Fokker-Planck equations that allow mapping to a stochastic simulation.

III. PROBLEMS WITH THE TRUNCATED WIGNER METHOD

The (single phase space) Wigner representation has been widely used to study diverse physical problems, with great success [13–15]. But a truncation of terms is necessary in most applications to allow a stochastic simulation. The truncated Wigner method is then not exact. Although the method gives good results in many cases, because the truncation of terms can be well justified if mode occupation numbers are large and simulation times are limited, the systematic errors can be significant if those conditions are not met. In addition, the estimation of a higher-order moment (the expectation of a product of more than one field operator) will generally contain a larger systematic error than the estimation of the expectation value of a single field operator [16].

Even when no truncation is necessary, there is the problem of large sampling error in a truncated Wigner simulation. While an initial coherent state can be represented by a positive-P distribution of zero width [see Eq. (4.10)], the same state will have a Wigner distribution with a finite width [Eqs. (2.11) and (2.12)]. For short times, the growing positive-P noise will not overtake the relatively constant Wigner noise. The result is greater sampling error in the Wigner simulation, requiring the calculation of far more trajectories to achieve the same precision.

The investigation of Deuar and Drummond [9] into BEC scattering showed how the truncation problem produces serious systematic errors in the simulation of a large number of interacting modes with many lightly occupied modes. We will discuss these problems later in this section.

Here we outline the reasons for truncation and the region of validity of the approximation.

From Eq. (2.3) it may be seen that the Wigner function is always real, but it may take negative values for some density matrices. This would prevent us from mapping our quantum mechanics problem to a stochastic simulation, since the latter would require a positive semidefinite quasiprobability distribution.

However, when we find the equation of motion for the Wigner function, the opportunity for an approximation procedure becomes apparent. This equation follows from the operator correspondences of the single Wigner representation [which can be obtained from Eqs. (2.7)–(2.10) with the replacement $\alpha^+ \rightarrow \alpha^*$] and the evolution equation for the density matrix

$$\frac{\partial \hat{\rho}}{\partial t} = -i[\hat{H}, \hat{\rho}]. \tag{3.1}$$

We are going to restrict our attention to Hamiltonians, including multimode Hamiltonians, that include products of creation and annihilation operators only up to quartic terms. This restriction will include the model of BECs with two-body s-wave scattering [17]. The equation for the evolution

TABLE I. Terms in the Fokker-Planck equation for a quartic Hamiltonian, using the Wigner and positive-P representations.

	Drift terms	Diffusion terms	Third-order terms
Wigner	Yes	No	Yes
Positive-P	Yes	Yes	No

of a Wigner function under such a Hamiltonian will always take the general form

$$\frac{\partial W}{\partial t} = -\frac{\partial}{\partial \alpha}[A(\alpha)W(\alpha)] - \frac{\partial}{\partial \alpha^*}[A^*(\alpha)W(\alpha)] + T_3. \tag{3.2}$$

Here T_3 is a term with three derivative operators, each either $\frac{\partial}{\partial \alpha}$ or $\frac{\partial}{\partial \alpha^*}$. The key point to note is that for undamped (unitary) time evolution, there are never any second-order (diffusion) terms, which is a consequence of the fact that the Wigner representation is symmetrically ordered. Also, fourth-order terms always cancel. These general results for quartic Hamiltonians, for the Wigner representation and for the positive-P representation, are summarized in Table I.

It is found that the third-order terms, including for more general multimode problems, may be truncated and produce a systematic error in $\frac{\partial W}{\partial t}$ that is relatively small compared to the other terms, in the limit that the occupation numbers of the modes remain very much greater than unity.

The motivation for this truncation is clear: Equation (3.2) then reduces to Liouville form, a special case of the Fokker-Planck equation in which only drift terms influence the evolution of the quasiprobability. If the initial density matrix for the problem is such that the Wigner function is everywhere non-negative (and this is a common situation) then the function will remain non-negative for all times. A further mapping to a stochastic simulation becomes possible. The only noise in the simulation will come from the initial condition, since no second-order terms are present to cause diffusion.

A small error in $\frac{\partial W}{\partial t}$ will produce a large error in W after a sufficiently long time, so this approximation procedure can only be valid for a finite time. Over the relevant time scales, the truncation is justified by a scaling argument. If the stochastic variable α is seen from the truncated equations of motion to remain of very large magnitude ($|\alpha| \sim \sqrt{N_0} \gg 1$), then we define a scaled variable $z = \alpha / \sqrt{N_0}$ and find that the third-order terms take the form

$$T_3 \sim \frac{1}{N_0} \partial \partial \partial(\zeta W), \tag{3.3}$$

where ∂ is either $\frac{\partial}{\partial z}$ or $\frac{\partial}{\partial z^*}$ and ζ is either z or z^*.

Deuar and Drummond [9] applied the truncated Wigner method to the large multimode problem of scattering BECs and found an ultraviolet divergence problem: Systematic errors that grow with the momentum cutoff imposed on the lattice. They were able to simulate a BEC collision with 150 000 bosons, using the positive-P representation for times long enough to obtain useful results, and thereby had an exact result to compare with the truncated Wigner method.

The latter method produced a "false halo" of particles in momentum space, depletion leading to unphysical negative densities beyond the halo, and accumulation of particles at low momenta—all in disagreement with the exact positive-P results. The Wigner method requires that initially empty modes of the system be represented by nonzero distributions, as if one-half of a virtual particle occupied each mode. Evidently the truncated Wigner method treats these virtual particles as if they were real, in that a scattering event involving them can produce real populations of product modes.

This is an ultraviolet divergence problem in that it becomes worse as the momentum cutoff is increased. To obtain the most physically relevant results from a simulation, one must extrapolate to the continuum limit. It is in this limit, as the momentum cutoff approaches infinity, that the truncation errors are divergent. Clearly a full Wigner-Moyal treatment without truncation would not have these errors, but such a full theory with third-order derivatives also involves negative probabilities, which have no stochastic equivalent.

We mention the projection method used with the truncated Wigner approach [18,19], which amounts to another way to implement a cutoff, but does not solve this ultraviolet divergence problem.

We mention here the projection methods as other techniques (not exact) for dealing with this problem.

This discussion of problems with the truncated Wigner method is given as motivation for a hybrid treatment. In future applications to multimode systems, we will investigate whether the hybrid method avoids these problems. The large number of initial vacuum modes in a collision, for example, would be treated in the hybrid method with the positive-P representation as phase-space variables set identically to zero. However, this requires a detailed future investigation. The problem is absent in the pure positive-P method, although at long times very large sampling errors are found instead [9].

IV. POSITIVE-P METHOD

The positive-P method involves an extension of the Glauber-Sudarshan P representation [20,21] from a single phase space to a doubled phase space, the same procedure that gives the doubled Wigner representation from the single. The defining equation (for a single-mode problem) gives a representation of the density matrix in terms of a c-number function, P, and nondiagonal projection operators, Λ_P, both defined on a doubled phase space,

$$\hat{\rho} = \int d^2\alpha \int d^2\alpha^+ P(\alpha, \alpha^+)\hat{\Lambda}_P(\alpha, \alpha^+), \quad (4.1)$$

with

$$\hat{\Lambda}_P(\alpha, \alpha^+) = \frac{|\alpha\rangle\langle\alpha^{+*}|}{\langle \alpha^{+*}|\alpha\rangle}. \quad (4.2)$$

Here $|\alpha\rangle$ indicates a coherent state: A normalized eigenstate of the annihilation operator $\hat{a}$. The effect of left-hand and right-hand multiplication of the density matrix by a and $a^\dagger$ on $P(\alpha, \alpha^+)$ can be deduced from Eqs. (4.1) and (4.2). The

proof involves an integration by parts in which boundary terms are assumed to vanish. The realm of validity of this assumption and the resulting effects on stochastic simulations are discussed at length by Gilchrist *et al.* [7]. When the boundary terms vanish, the operator correspondences are

$$\hat{a}\hat{\rho} \leftrightarrow \alpha P(\alpha, \alpha^+), \quad (4.3)$$

$$\hat{\rho}\hat{a} \leftrightarrow \left(\alpha - \frac{\partial}{\partial\alpha^+}\right)P(\alpha, \alpha^+), \quad (4.4)$$

$$\hat{a}^\dagger\hat{\rho} \leftrightarrow \left(\alpha^+ - \frac{\partial}{\partial\alpha}\right)P(\alpha, \alpha^+), \quad (4.5)$$

$$\hat{\rho}\hat{a}^\dagger \leftrightarrow \alpha^+ P(\alpha, \alpha^+). \quad (4.6)$$

As we have noted in Table I, all quartic Hamiltonian problems, in the positive-P representation, give a true Fokker-Planck equation, with at most drift and diffusion terms,

$$\frac{\partial P}{\partial t} = -\partial_\mu[A^\mu(\alpha, \alpha^+)P] + \frac{1}{2}\partial_\mu\partial_\nu[D^{\mu\nu}(\alpha, \alpha^+)P], \quad (4.7)$$

with

$$\partial_1 = \frac{\partial}{\partial\alpha}, \quad \partial_2 = \frac{\partial}{\partial\alpha^+}, \quad (4.8)$$

and summation over μ, ν implied. Thus, for the many-boson Hamiltonian with two-body s-wave scattering terms [17], no truncation of the positive-P equations is needed.

The positive-P method solves two problems that occur with single phase-space representations. First, if the distribution function is not guaranteed to remain real and non-negative, we cannot map the dynamics onto a stochastic simulation using standard methods. To deal with this, we use the feature of the representation that an infinity of different functions, $P(\alpha, \alpha^+)$, may represent the same density matrix. We may choose, for the initial condition, a particular function

$$P_+(\alpha, \alpha^+) = \frac{1}{4\pi^2}e^{-1/4|\alpha - \alpha^{+*}|^2}\left\langle \frac{1}{2}(\alpha + \alpha^{+*})\left|\hat{\rho}\right|\frac{1}{2}(\alpha + \alpha^{+*})\right\rangle,$$
$$(4.9)$$

that satisfies Eq. (4.1) and is everywhere non-negative, as required. Alternatively, an initial pure coherent state, with $\hat{\rho} = |\gamma\rangle\langle\gamma|$, can have a δ-function representation, also positive,

$$P(\alpha, \alpha^+) = \delta^2(\alpha - \gamma)\delta^2(\alpha^+ - \gamma^*). \quad (4.10)$$

The stochastic representation of this initial condition is simply

$$\alpha = \gamma, \quad \alpha^+ = \gamma^*. \quad (4.11)$$

The second problem to deal with is that the diffusion matrix may not be positive semidefinite when written in the basis of real (x) and imaginary (y) parts $(\alpha_x, \alpha_x^+, \alpha_y, \alpha_y^+)$. However, there is another symmetry in the positive-P representation, arising from the analyticity in α and α^+ of the nondiagonal projection operator (4.2), that lets us make re-

placements to the real and imaginary parts of the derivative operators (4.8) in (4.3)–(4.6), in just such a way that the resulting Fokker-Planck equation, relative to the component basis, has a positive semidefinite diffusion matrix [8]. With a positive initial condition and a true, positive semidefinite Fokker-Planck equation, the distribution is guaranteed to remain positive. The standard method of mapping to a stochastic simulation also requires a diffusion matrix that is positive semidefinite (all of its eigenvalues are non-negative), so that stochastic equations are immediately derivable.

The final step of mapping to stochastic differential equations involves first finding an N-noise factorization of the diffusion matrix of the form

$$D^{\mu\nu} = \sum_{n=1}^{N} B^{\mu n} B^{\nu n}. \tag{4.12}$$

This introduces another gauge degree of freedom that we will exploit later. Different choices of the factor matrix, B, that satisfy (4.12) may provide stochastic simulations with widely different sampling error characteristics.

The result of the adjustment of the diffusion matrix and this choice of the factor matrix is the set of Itô stochastic differential equations

$$d\alpha^{\mu} = A^{\mu} dt + \sum_{n=1}^{N} B^{\mu n} dw_n, \tag{4.13}$$

where the dw_n are N real Weiner increments [8] satisfying the stochastic average

$$\langle\langle dw_n(t) dw_m(t) \rangle\rangle = \delta_{nm} dt. \tag{4.14}$$

These SDEs, with appropriate initial conditions [Eqs. (4.11) for coherent states], are used to evolve a large ensemble of trajectories. The positive-P representation is normally ordered, meaning that the most easily calculated quantum-mechanical expectation values are of normally ordered operators. The formula for estimating a normally ordered quantum-mechanical expectation value as a stochastic average is

$$\langle \hat{a}^{\dagger m} \hat{a}^n \rangle = \langle\langle \alpha^{+m} \alpha^n \rangle\rangle. \tag{4.15}$$

We see from Eq. (4.11) that a coherent state can be represented initially with no noise in the positive-P representation. In this paper we will not embark on a detailed comparison of sampling error in the truncated Wigner, positive-P and hybrid methods. However, we will take note of the number of trajectories needed, in each method, for an ensemble average to converge to a satisfactory result. All of our simulations were performed using xmds [22], and we used the built-in sampling error estimates of that program to judge convergence.

The next part of our construction of the hybrid representation involves writing the nondiagonal projectors for the positive-P representation in normally ordered Gaussian form. The result of manipulating Eq. (4.2) is

$$\Lambda_P(\alpha, \alpha^+) = :e^{-(\hat{a}^{\dagger} - \alpha^+)(\hat{a} - \alpha)}:. \tag{4.16}$$

V. PROBLEMS WITH THE POSITIVE-*P* METHOD

A particular choice of the factor matrix, B, gives a set of stochastic differential Eqs. (4.13) that governs the evolution of the ensemble of trajectories. Unless this evolution is constrained in some way, trajectories may wander far from each other in phase space. Then the averaging over trajectories to estimate an expectation value may involve additions of many different, extremely large, numbers. No computer can calculate such an average without incurring a very large round-off error.

The result is the dramatic rise in sampling error that has been seen in some positive-P simulations. The growth in width of the distribution of trajectories often occurs over a short time scale, so that the sampling error suddenly rises by many orders of magnitude, with the resulting growth of numerical errors. The simulation is of no value beyond this critical time.

The problem can be caused by drift terms or noise terms, or a combination of both. A single-mode example to illustrate these problems is the anharmonic oscillator, with Hamiltonian

$$\hat{H} = \omega \hat{a}^{\dagger} \hat{a} + \chi \hat{a}^{\dagger} \hat{a}^{\dagger} \hat{a} \hat{a} \tag{5.1}$$

and positive-P Itô stochastic differential equations,

$$d\alpha = -i(\omega + 2\chi \alpha^+ \alpha)\alpha dt + \sqrt{-2i\chi} dw, \tag{5.2}$$

$$d\alpha^+ = +i(\omega + 2\chi \alpha^+ \alpha)\alpha^+ dt + \sqrt{2i\chi} dw^+. \tag{5.3}$$

If we ignore the noise terms and choose $\alpha^+\alpha$ as a real number initially, the trajectory will be a circle in the complex α plane. But if $\alpha^+\alpha$ includes an imaginary part [from noise or from an initial condition other than the coherent state condition (4.11)], either α or α^+ will spiral toward infinity, while the other spirals in toward the origin. The noise terms of the SDEs contribute to the problem, since they generally move $\alpha^+\alpha$ away from real values, thereby inducing the spiraling.

Note that the single Wigner representation does not suffer from this problem because the real term $|\alpha|^2$ will always appear in place of $\alpha^+\alpha$ in the SDEs.

Sampling error growth can be reduced or postponed by using our freedom to choose different factor matrices that give the same diffusion matrix, and by modifying the drift equations. Such methods are called stochastic gauge techniques [23–25]. However, while these are useful in single-mode examples, they are somewhat complicated when generalized to multimode cases. Also, we are interested in extending the time available for useful, error-free simulations to even longer time scales than these methods can provide.

A special case of problems with drift trajectories is when a trajectory is capable of reaching infinity in a finite time [7]. This typically results in power-law tails in the distribution function, which violates the assumption that partial integration can be carried out. The simulation as it stands is then invalid beyond the singularity time. This problem can be dealt with using drift gauges [23]. Our examples will not fit into this category.

We simulated the anharmonic oscillator in the positive-P representation to illustrate the sampling error problem. Fig-
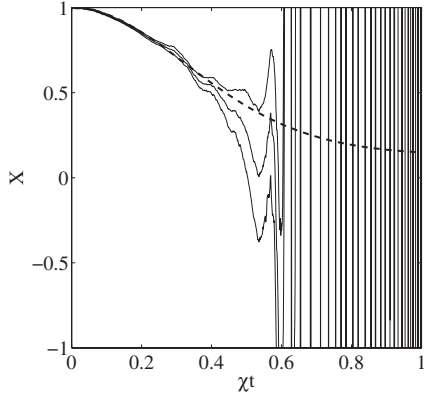
FIG. 1. X quadrature for single-mode anharmonic oscillator vs χt: Positive-P method. Plotted are the ensemble average and the ensemble average $\pm$ sampling error estimate. The dashed line is the exact result. Parameters: $\omega = 0$, $N_0 = 1$. Number of trajectories: 1000.

ure 1 shows the X quadrature [$\hat{X} = \frac{1}{2}(\hat{a} + \hat{a}^\dagger)$], with the choices $\omega = 0$ (for simplicity) and initial average number $N_0 = 1$. As we will do for all of our simulations, we plot results against a scaled time parameter, in this case χt. (This is dimensionless when using $\hbar = 1$.)

Deuar and Drummond [23] have investigated various factors that affect the time for sampling error to become unmanageable in a multimode positive-P simulation. They have found that coarser spatial lattices, weaker interactions, and lower particle densities all extend the lifetime of the simulation. Of course the spatial lattice spacing can only be increased at the expense of systematic error, while the other two factors are fixed by the system being simulated.

In the hybrid scheme we will be using the positive-P representation only for the modes with lowest occupations. Our test cases will investigate whether this delays the onset of large sampling error.

VI. HYBRID METHOD

The hybrid method is designed to exploit a particular feature of Bose-Einstein condensate systems: A limited number of modes have very high occupation numbers. The method involves separating the physical system into modes that are, at least initially, highly occupied (the condensed modes) and those that are lightly occupied (the output of an atom laser or the products of a BEC collision). Then we intend to use different representations to treat different modes, treating the highly occupied modes with a form of the Wigner representation and the lightly occupied modes with the positive-P representation.

Use of the Wigner representation for the highly occupied modes will in general simplify the structure of the resulting diffusion matrix. In a simple two-mode model discussed in Sec. VII, we will see that this allows us to delay the rapid growth of sampling error. Also, by not using the Wigner representation for the potentially very large number of lightly occupied modes, we intend to avoid the false halo problem.

Our first task is to show that we can consistently use two different representations on different modes, correctly de-

scribing interactions that couple these different modes. For general interactions of this sort, diffusion terms involving the Wigner modes are inevitable. To be able to construct a positive semidefinite diffusion matrix in the general case, we must use a doubled phase space throughout.

Now we can exploit the similarities in Eqs. (2.6) and (4.16) to define a hybrid representation with a particularly simple notation. We suppose that a system has modes labeled $m = 1, \ldots, M$. These modes are to be treated with the Wigner representation or the positive-P representation depending on whether a parameter r_m takes the value

$$r_m = 1 \quad \text{for positive-P,} \tag{6.1}$$

$$r_m = 2 \quad \text{for Wigner.} \tag{6.2}$$

The nondiagonal projection operator is a direct product of terms for each mode, m,

$$\hat{\Lambda}_H(\vec{\alpha}; \vec{r}) = \prod_{m=1}^{M} r_m : e^{-r_m(\hat{a}^\dagger - \alpha^+)(\hat{a} - \alpha)} : . \tag{6.3}$$

Then the hybrid representation of the density matrix becomes

$$\hat{\rho} = \int d^{4M} \vec{\alpha} \, P_H(\vec{\alpha}; \vec{r}) \hat{\Lambda}_H(\vec{\alpha}; \vec{r}), \tag{6.4}$$

where $\vec{\alpha} = (\alpha_1, \alpha_1^+, \ldots, \alpha_M, \alpha_M^+)$ and $\vec{r} = (r_1, \ldots, r_M)$.

Note that the use of the parameter r for these doubled phase-space representations is very much like the Glauber and Cahill use of the parameter s to span antinormally ordered, symmetrically ordered, and normally ordered single phase-space representations. The connection between the two schemes follows by taking

$$r = \frac{s - 1}{s} \tag{6.5}$$

and mapping doubled to single phase spaces.

The applicability of the positive-P method depends on the two results that we mentioned in Sec. IV. First, for any initial density matrix, it is possible to choose a phase-space distribution that is everywhere real and non-negative [using Eq. (4.9)]. Second, it is always possible to cast any diffusion matrix into a form that is equivalent with respect to physical predictions and that is positive semidefinite in the basis of real and imaginary parts of the phase-space variables. Corresponding results must hold for any hybrid representation in order for that method to be usable. We were able to prove both assertions.

First, we found an integral transform that takes a positive-P distribution to a doubled Wigner distribution representing the same density matrix. We show the single-mode case,

$$\mathcal{W}(\alpha, \alpha^+) = \frac{1}{2\pi} \int d^2\psi' \, e^{-1/2|\psi - \psi'|^2} P\left(\frac{1}{2}(\psi' + \chi), \frac{1}{2}(\psi' - \chi)\right), \tag{6.6}$$

with

$$\psi = \alpha + \alpha^{+*}, \quad \chi = \alpha - \alpha^{+*}. \tag{6.7}$$

Note that P has four independent real parameters, but the integration is over only two degrees of freedom. The single-mode case is shown but the extension to the multimode case is straightforward. Since the kernel is positive, the transform can be used to take the initial positive distribution (4.9) to an everywhere positive doubled Wigner distribution. Extension to the case with many modes treated by different representations proves the first assertion.

The proof of the second assertion is exactly like the textbook proof for the positive-P representation, since the derivative equivalences

$$\frac{\partial}{\partial \alpha} \leftrightarrow \frac{\partial}{\partial \alpha_x} \leftrightarrow -i \frac{\partial}{\partial \alpha_y}, \tag{6.8}$$

$$\frac{\partial}{\partial \alpha^+} \leftrightarrow \frac{\partial}{\partial \alpha_x^+} \leftrightarrow -i \frac{\partial}{\partial \alpha_y^+}, \tag{6.9}$$

are the same as their positive-P counterparts.

Use of the hybrid method is simple for few-mode problems. For the mapping of the evolution Eq. (3.1) for ρ to a Fokker-Planck equation, we use either the Wigner (2.7)–(2.10) or positive-P (4.3)–(4.6) operator correspondences as appropriate for each mode. In general there will be terms with three derivative operators for quartic Hamiltonians. (Terms with four derivatives always cancel.) For each application, we must decide whether truncation of these terms, to produce a drift or diffusion problem, is valid. Scaling arguments such as those applied to the Wigner method (3.3) can be used here. In problems involving both highly occupied modes and lightly occupied modes, there may occur problematic three-derivative terms from mutual interaction of those modes.

A feature peculiar to the hybrid method is that there will appear what we call interface noise: There will be diffusion terms that are proportional to the difference of r values for different modes, that would vanish if those modes were treated with the same representation.

The mapping to stochastic differential equations uses the same rule as is used for the positive-P representation: If a generally complex matrix B provides a factorization $D = BB^T$ of the diffusion matrix, then the Itô stochastic differential equations can be chosen as

$$d\alpha^\mu = A^\mu dt + \sum_{n=1}^{N} B^{\mu n} dw_n, \tag{6.10}$$

where μ labels the components of the vector of phase-space variables $\vec{\alpha} = (\alpha_1, \alpha_1^+, \ldots, \alpha_M, \alpha_M^+)$ and the dw_n are N real, independent Weiner increments. We note that the freedom of choice of a factor matrix, B, introduces a gauge degree of freedom that may allow us to reduce sampling error in simulations.

The relation between physical expectation values and stochastic averages will take new forms in the hybrid representation. Here an observable may be a product of factors to be treated with the symmetrically ordered Wigner representation and others to be treated with the normally ordered positive-P

representation. So, for example, in Sec. IX we will need to calculate an expectation value as

$$\langle \hat{N}_a \hat{Y}_b \rangle = \left\langle \frac{1}{2i} \hat{a}^\dagger \hat{a} (\hat{b} - \hat{b}^\dagger) \right\rangle = \left\langle \left\langle \frac{1}{2i} \left(\alpha^+ \alpha - \frac{1}{2} \right) (\beta - \beta^\dagger) \right\rangle \right\rangle, \tag{6.11}$$

where the a mode is treated with the Wigner representation while the b mode is treated with the positive-P representation.

VII. TEST CASE: COUPLED ANHARMONIC OSCILLATORS

As a first test of the hybrid method, we simulated the behavior of two coupled anharmonic oscillators, with a coupling that preserves the individual mode occupations. The Hamiltonian is

$$\hat{H} = \omega_a \hat{a}^\dagger \hat{a} + \chi_a \hat{a}^\dagger \hat{a}^\dagger \hat{a} \hat{a} + \omega_b \hat{b}^\dagger \hat{b} + \chi_b \hat{b}^\dagger \hat{b}^\dagger \hat{b} \hat{b} + g \hat{a}^\dagger \hat{a} \hat{b}^\dagger \hat{b}. \tag{7.1}$$

We used an initial coherent state for the a mode (with high mean occupation $N_{a0} = 100$) and for the b mode (low mean occupation $N_{b0} = 0.01$). We set $\omega_a = \omega_b = 0$ for convenience and used $\chi_a = \chi_b = g = 1$, which sets the scale for the time variable.

This model is meant to resemble just a few terms of the much larger multimode Hamiltonian for a Bose gas with s-wave scattering terms.

Note that we have chosen a model system in which the a occupation remains constantly large, while the b occupation stays small. The hybrid method can be used in cases where these numbers are not conserved, and gives good results when the occupations of the modes remain high and low over the interaction time, respectively. Results from this category will be presented in a later work.

We simulated this system using the hybrid method and, for comparison, the truncated Wigner method and the positive-P method. We were also able to obtain an exact solution for coherent state initial conditions, as did Chaturvedi and Srinivasan [26].

We insert the hybrid representation (6.4) of the density matrix into the evolution equation (3.1). An integration by parts, justified in this case, amounts to using the hybrid operator correspondences [(2.7)–(2.10) and (4.3)–(4.6)]. This gives an equation of the form

$$\int d^8 \vec{\alpha} \frac{\partial P_H}{\partial t} \hat{\Lambda}_H(\vec{\alpha}, \vec{r}) = \int d^8 \vec{\alpha} \mathcal{L}(\vec{\alpha}, \vec{r}) P_H(\vec{\alpha}, \vec{r}) \hat{\Lambda}_H(\vec{\alpha}, \vec{r}), \tag{7.2}$$

where $\mathcal{L}$ is a linear, differential operator that acts on P_H.

We extract a Fokker-Planck equation for P_H from (7.2), keeping all terms, including third-order derivative terms. (We note that for doubled phase-space representations this choice is not unique.). We find

$$i\frac{\partial P_H}{\partial t} = -\frac{\partial}{\partial \alpha}\{2\chi_a(\alpha^+\alpha - 1) + g\beta^+\beta\}\alpha P_H$$

$$+ \frac{\partial}{\partial \alpha^+}\{2\chi_a(\alpha^+\alpha - 1) + g\beta^+\beta\}\alpha^+ P_H$$

$$- \frac{\partial}{\partial \beta}\left\{2\chi_b\beta^+\beta + g\left(\alpha^+\alpha - \frac{1}{2}\right)\right\}\beta P_H$$

$$+ \frac{\partial}{\partial \beta^+}\left\{2\chi_b\beta^+\beta + g\left(\alpha^+\alpha - \frac{1}{2}\right)\right\}\beta^+ P_H + \chi_b\frac{\partial^2}{\partial \beta^2}\beta^2 P_H$$

$$- \chi_b\frac{\partial^2}{\partial \beta^{+2}}\beta^{+2}P_H + \frac{g}{2}\frac{\partial}{\partial \alpha}\frac{\partial}{\partial \beta}\alpha\beta P_H + \frac{g}{2}\frac{\partial}{\partial \alpha}\frac{\partial}{\partial \beta^+}\alpha\beta^+ P_H$$

$$- \frac{g}{2}\frac{\partial}{\partial \alpha^+}\frac{\partial}{\partial \beta}\alpha^+\beta P_H - \frac{g}{2}\frac{\partial}{\partial \alpha^+}\frac{\partial}{\partial \beta^+}\alpha^+\beta^+ P_H$$

$$+ \frac{g}{4}\frac{\partial}{\partial \alpha}\frac{\partial}{\partial \alpha^+}\left\{\frac{\partial}{\partial \beta}\beta - \frac{\partial}{\partial \beta^+}\beta^+\right\}P_H + \frac{\chi_a}{2}\left\{\frac{\partial^2}{\partial \alpha^2}\frac{\partial}{\partial \alpha^+}\alpha\right.$$

$$\left. - \frac{\partial^2}{\partial \alpha^{+2}}\frac{\partial}{\partial \alpha}\alpha^+\right\}P_H. \tag{7.3}$$

We use the convention that the derivative operators act on all factors to the right-hand side.

To apply the scaling argument discussed in Sec. III, we write the third-order derivative terms above (which we call T_3) in terms of the scaled phase-space variables

$$u \equiv \alpha/\sqrt{N_{a0}}, \quad u^+ \equiv \alpha^+/\sqrt{N_{a0}}, \tag{7.4}$$

$$v \equiv \beta/\sqrt{N_{b0}}, \quad v^+ \equiv \beta^+/\sqrt{N_{b0}}. \tag{7.5}$$

Then T_3 becomes

$$T_3 = \frac{1}{N_{a0}}\frac{g}{4}\frac{\partial}{\partial u}\frac{\partial}{\partial u^+}\left\{\frac{\partial}{\partial v}v - \frac{\partial}{\partial v^+}v^+\right\}P_H$$

$$+ \frac{1}{N_{a0}}\frac{\chi_a}{2}\left\{\frac{\partial^2}{\partial u^2}\frac{\partial}{\partial u^+}u - \frac{\partial^2}{\partial u^{+2}}\frac{\partial}{\partial u}u^+\right\}P_H. \tag{7.6}$$

We expect, in the stochastic simulation of this problem, that there will be a finite time scale over which α and α^+ will remain distributed close to order $\sqrt{N_{a0}}$ in magnitude, while β and β^+ remain near $\sqrt{N_{b0}}$. Our first simulation will stay within this time region. Over that time scale, the third-order derivative terms will make a negligible contribution to P_H compared to the drift terms (first-order terms which scale as N_{a0}) and the diffusion terms (second-order terms which scale as 1).

After we truncate these terms, the Fokker-Planck equation has drift vector [in the basis $(\alpha, \alpha^+, \beta, \beta^+)$]

$$A = \begin{pmatrix} -i\{2\chi_a(\alpha^+\alpha - 1) + g\beta^+\beta\}\alpha \\ +i\{2\chi_a(\alpha^+\alpha - 1) + g\beta^+\beta\}\alpha^+ \\ -i\left\{2\chi_b\beta^+\beta + g\left(\alpha^+\alpha - \frac{1}{2}\right)\right\}\beta \\ +i\left\{2\chi_b\beta^+\beta + g\left(\alpha^+\alpha - \frac{1}{2}\right)\right\}\beta^+ \end{pmatrix} \tag{7.7}$$
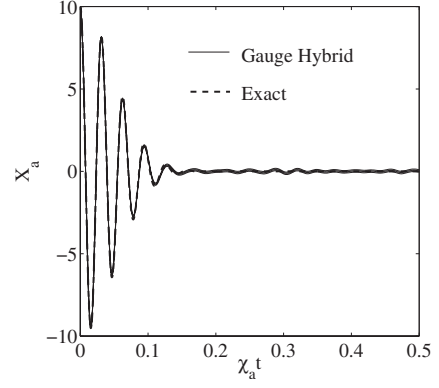
and diffusion matrix

FIG. 2. X quadrature for mode a vs $\chi_a t$: Coupled anharmonic oscillators treated with the gauge hybrid method. Plotted are the ensemble average, the ensemble average $\pm$ sampling error estimate, and the exact solution. Parameters: $\omega_a = \omega_b = 0$, $\chi_a = \chi_b = g$, $N_{a0} = 100$, $N_{b0} = 0.01$. Number of trajectories: 10 000.

$$D = \begin{pmatrix} 0 & 0 & -\frac{ig}{2}\alpha\beta & -\frac{ig}{2}\alpha\beta^+ \\ 0 & 0 & +\frac{ig}{2}\alpha^+\beta & +\frac{ig}{2}\alpha^+\beta^+ \\ -\frac{ig}{2}\alpha\beta & +\frac{ig}{2}\alpha^+\beta & -2i\chi_b\beta^2 & 0 \\ -\frac{ig}{2}\alpha\beta^+ & +\frac{ig}{2}\alpha^+\beta^+ & 0 & +2i\chi_b\beta^{+2} \end{pmatrix}. \tag{7.8}$$

Because of the use of the Wigner representation for the a mode, this diffusion matrix differs from the one resulting from a pure positive-P treatment in the absence of terms $-2i\chi_a\alpha^2$ and $+2i\chi_a\alpha^{+2}$ in the first two diagonal spaces, respectively.

We were able to construct a factorization of the diffusion matrix (7.8) by first treating the diagonal terms and then recognizing a simple structure in the remaining matrix. The following factor matrix requires only four real noises in the SDEs:

$$B = \sqrt{2i\chi_b}\begin{pmatrix} 0 & 0 & 0 & 0 \\ 0 & 0 & 0 & 0 \\ i\beta & 0 & 0 & 0 \\ 0 & \beta^+ & 0 & 0 \end{pmatrix} + \frac{1}{2}\sqrt{-ig}\begin{pmatrix} 0 & 0 & \alpha & i\alpha \\ 0 & 0 & -\alpha^+ & -i\alpha^+ \\ 0 & 0 & \beta & -i\beta \\ 0 & 0 & \beta^+ & -i\beta^+ \end{pmatrix}. \tag{7.9}$$

The resulting SDEs produced the results shown in Figs. 2 and 3. We calculated the expectation values of the quadrature operators $\hat{X}_a = \frac{1}{2}(\hat{a} + \hat{a}^\dagger)$ and $\hat{X}_b = \frac{1}{2}(\hat{b} + \hat{b}^\dagger)$. The simulation was clearly stable over the time scale shown and gave results in excellent agreement with the exact solution. We will refer to the method used here as a gauge hybrid method, since it relies on being able to find a diffusion gauge (a useful factorization of the diffusion matrix).
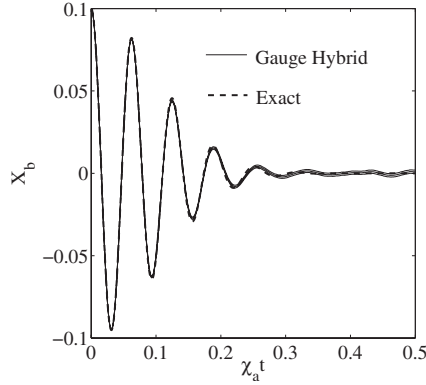
FIG. 3. X quadrature for mode b vs $\chi_a t$: Coupled anharmonic oscillators treated with the gauge hybrid method. Plotted are the ensemble average, the ensemble average $\pm$ sampling error estimate, and the exact solution. Parameters: $\omega_a = \omega_b = 0$, $\chi_a = \chi_b = g = 1$, $N_{a0} = 100$, $N_{b0} = 0.01$. Number of trajectories: 10 000.

When we simulated this same problem using the truncated Wigner method, the results were nearly indistinguishable from Figs. 2 and 3 (using 150 000 trajectories), so we do not display them here. With regard to this first test, we have not yet established superiority of the hybrid method over the truncated Wigner, except to note that the hybrid method requires far fewer trajectories to attain a given accuracy. In Sec. VIII we will explore a different region of parameter space and in Sec. X we will calculate a higher-order moment in the same system. In both cases, we will see results that show a clear distinction between the methods.

We also simulated this problem with the positive-P method. Sampling error increased to very large values at about $\chi_a t = 0.04$, after just one oscillation of the quadratures.

Analysis of the third-order derivative terms from the pure Wigner calculation, similar to the above analysis for the hybrid method, shows terms that scale as $1/N_{b0}$ and so cannot be justifiably neglected.

The mechanism at work in stabilizing the hybrid simulation over limited times is as follows. With this choice of gauge, the stochastic differential equations keep the quantity $\alpha^+ \alpha$ fixed, for each trajectory, at its initial value. These values, selected by the stochastic Wigner initial condition of the form (2.11) and (2.12), will always be real and close to N_{a0}. The quantity $\beta^+ \beta$ starts at N_{b0} then acquires an imaginary part, but its magnitude is kept of order N_{b0} over the simulation time.

Further inspection shows that the magnitudes of α and α^+ will remain near $\sqrt{N_{a0}}$ while those of β and β^+ remain of the order of $\sqrt{N_{b0}}$ over the simulation time. [These estimates were used to justify our neglect of the third-order derivative terms in Eqs. (7.4)–(7.6).] So the drift terms are dominated by the factors of $\alpha^+ \alpha$ and spiraling is negligible.

Over a short time Δt, the relative sizes of the drift and diffusion increments, for z one of the phase-space variables, are given by

$$\text{Drift:} \quad \Delta z \sim N_a z \Delta t,$$

$$\text{Diffusion:} \quad \Delta z \sim z \sqrt{\Delta t}$$

(with $\chi_a = \chi_b = g = 1$). So diffusion is, in this example, negligible compared to drift over the time scale of interest.
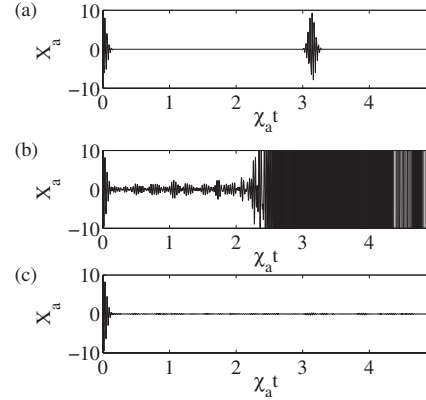

FIG. 4. X quadrature for mode a calculated to longer (dimensionless) times $\chi_a t$. (a) Exact result. (b) Gauge hybrid result: 100 trajectories. (c) Truncated Wigner result: 10 000 trajectories. Parameters: $\omega_a = \omega_b = 0$, $\chi_a = \chi_b = g$, $N_{a0} = 100$, $N_{b0} = 0.01$.

We calculated the quadrature X_a in our model to longer times, with results shown in Fig. 4. (To obtain the qualitative features rapidly, we used, in each case, a lower number of trajectories than we used in our previous simulations.) The exact result showed a recurrence centered on $\chi_a t = \pi$. The gauge hybrid method showed large sampling error before that time, starting at about $\chi_a t = 2.5$. The truncated Wigner method was also unable to predict this recurrence, showing instead a quadrature remaining close to zero. Recalling that the pure positive-P treatment suffered large sampling error after about $\chi_a t = 0.04$, we see that the gauge hybrid method extended the useful simulation time by a factor of 60.

VIII. WEAK COUPLING

In the previous example, both the gauge hybrid method and the truncated Wigner method are aided by the fact that the quadratures are strongly damped before the neglect of terms (for both methods) and sampling error growth (for the hybrid method) can become important. We lowered the mutual interaction strength between the two modes, relative to $\chi_a = \chi_b$, by setting $g/\chi_a = 0.0001$. This greatly extended the damping time for the b mode, allowing us to see differences in the predictions of the gauge hybrid and truncated Wigner methods.

The results are shown in Fig. 5.

We see that the truncated Wigner method fails from $\chi_a t = 0$, consistent with our expectations for a system with a very lightly occupied mode. The gauge hybrid method performs well until about $\chi_a t = 1.5$, when it is overwhelmed by sampling error.

IX. FURTHER TRUNCATION

In the examples we have seen so far, truncation of terms in the hybrid method has not prevented it from attaining excellent agreement with the exact solutions at early times, even when dealing with a very lightly occupied mode. The method is, however, clearly limited by the growth of sampling error. In this section, we try a simple adjustment to the
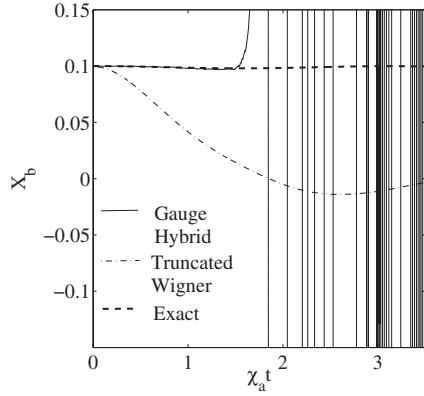
FIG. 5. Comparison of the gauge hybrid and truncated Wigner methods in predicting the X quadrature for the b mode of the coupled anharmonic oscillators, with weak coupling. Quadratures plotted against $\chi_a t$. Gauge hybrid result: 10 000 trajectories. Truncated Wigner result: 15 000 trajectories. Parameters: $\omega_a = \omega_b = 0$, $\chi_a = \chi_b$, $g/\chi_a = 0.0001$, $N_{a0} = 100$, $N_{b0} = 0.01$.

equations to try to extend useful results to longer times.

When phase-space distributions grow wide in unconstrained directions, the trajectories sampling those distributions are widely spread and the calculation of expectation values becomes a great numerical difficulty. To understand the meaning of the widths in "unconstrained directions," we note that we could estimate the spread of our hybrid distribution by calculating all the stochastic averages $\langle\langle \alpha^i \alpha^j \rangle\rangle$, where α^i is a real or imaginary part of $\vec{\alpha}$ [defined after Eq. (6.10)]. Some of the linear combinations of these averages, such as $\langle\langle \alpha^+ \alpha \rangle\rangle$, are constrained to approach physical predictions as the number of trajectories grows large. Widening of the distribution in the other directions will increase sampling error, but may be reduced using the gauge freedoms of doubled phase-space representations, or other methods.

Spiraling of the drift trajectories is one source of spreading that we have identified, and that we have already partially controlled using our choice of gauge. For our gauge SDEs, the quantity $\alpha^+ \alpha$ remains completely real for all times, and thus does not cause spiraling in the drift equations. This is not the case for the quantity $\beta^+ \beta$, which starts with a purely real value but can immediately develop an imaginary part from the influence of the noise terms.

We tried a further truncation of our gauge hybrid equations, making the replacement

$$\beta^+ \beta \rightarrow \mathrm{Re}(\beta^+ \beta). \tag{9.1}$$

In future applications, if $\alpha^+ \alpha$ is not constrained, we propose to also try the truncation

$$\alpha^+ \alpha \rightarrow \mathrm{Re}(\alpha^+ \alpha). \tag{9.2}$$

We find good short-time behavior from this truncated hybrid method, equaling that of all the other methods. At longer times the method was unable to predict the recurrence, showing quadratures staying close to zero. But the sampling error remained at a manageable level to $\chi_a t = 5.0$. In future work, we will investigate whether this somewhat *ad-hoc* truncation can be used as a simple way to extend simulations to longer

times without incurring excessive systematic error.

X. TEST CASE: QUANTUM NONDEMOLITION MEASUREMENT

Our first test case showed the hybrid method—with a diffusion gauge choice and with a further truncation—able to successfully simulate an interacting system beyond the time at which the positive-P method became unusable. But the Wigner method was able to give equally good results on the same system. (A distinction was found in the weak coupling case.) Here we investigate a different observable—a higher-order moment—in the same system, and find the results more sensitive to the choice of method.

The concept of quantum nondemolition measurements [27,28] began with the need for a way to measure the very small displacements of a gravitational wave detector that are expected to occur from the passage of a gravitational wave. Repeated measurements of position, to high accuracy, would be required to distinguish the signal from other effects. Quantum mechanics sets limits on schemes to measure those small displacements. Measurement of a position observable with a finite uncertainty may produce a state in which the uncertainty in position grows after the measurement. At later times, when another measurement of position is performed, the uncertainty would be larger that the desired maximum.

Instead, measurement of a conserved observable, such as the momentum of a free particle, can be repeated an arbitrary number of times without causing the uncertainty to increase. The quantum nondemolition (QND) measurement scheme involves choosing an appropriate conserved observable (in a probe beam) that can give information about the signal of interest after the signal and probe interact.

A QND scheme can be constructed from our model of interacting anharmonic oscillators [29]. We suppose that the bosons in question are now photons, and that they can interact with each other in a suitable nonlinear medium, such that our number-conserving interaction Hamiltonian gives a toy model of the dynamics. Of course a fuller description of the dynamics would involve propagation in space, dispersion, and other factors [30]. A lightly occupied signal beam and a highly occupied probe beam interact in the medium. Phase information will be exchanged between them, while their individual number distributions are conserved.

In one QND scheme, the conserved QND observable is taken as the photon number, $\hat{N}_a$, in the highly occupied probe beam. The signal is the phase quadrature of the lightly occupied beam, $\hat{Y}_b = -\frac{i}{2}(\hat{b}^\dagger - \hat{b})$.

We suppose that the interaction between signal and probe lasts only for a short time, as would be the case for two short pulses interacting in an optical fiber. We make the interaction cease when the magnitude of the correlation function reaches its first maximum. This means that we use the previous Hamiltonian of Eq. (7.1), except with $g = 1$ for $t < t_0$, and $g = 0$ for $t > \chi_a t_0$, where $\chi_a t_0 = 0.1$ in our example.

We calculate the correlation function between probe and signal, a measure of the potential success of the measurement scheme,
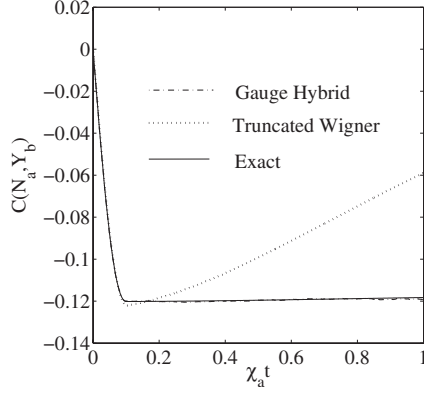
FIG. 6. Comparison of methods for determining the correlation between N_a and Y_b for a QND scheme vs $\chi_a t$. Results are shown for the hybrid method with a diffusion gauge (50 000 trajectories) and the truncated Wigner method (50 000 trajectories), compared to the exact result. Parameters: $N_{a0}=100$, $N_{b0}=0.01$, $\omega_a=0$, $\omega_b=-N_{a0}g$, $\chi_a=\chi_b$, $g/\chi_a=1$ for $\chi_a t < 0.1$, $g=0$ for $\chi_a t > 0.1$.

$$C(N_a, Y_b) = \frac{\langle \hat{N}_a \hat{Y}_b \rangle - \langle \hat{N}_a \rangle \langle \hat{Y}_b \rangle}{V^{1/2}(N_a) V^{1/2}(Y_b)}, \qquad (10.1)$$

where

$$V(\hat{\Omega}) = \langle \hat{\Omega}^2 \rangle - \langle \hat{\Omega} \rangle^2 \qquad (10.2)$$

is the variance of an operator $\hat{\Omega}$. We set $\omega_a=0$ for convenience, since this will remove a high-frequency variation from our expectation value. Likewise, we set $\omega_b=-N_{a0}g$ to obtain a slowly varying expectation value. This latter choice is equivalent to a particular choice of local oscillator frequency in the homodyne detection of Y_b.

Figure 6 shows the correlation function calculated with two different phase-space methods and compared to the exact result. The gauge hybrid method shows excellent agreement with the exact result. In contrast, the truncation of the Wigner method evidently removes terms that are needed to correctly predict the correlation function at times after the interaction ceases. The tendency of the truncated Wigner method to give worse results when predicting higher-order moments was investigated by Drummond *et al.* [16].

XI. CONCLUSIONS

We have shown that, for a stochastic phase-space treatment of a multimode system, it is possible to use the doubled Wigner representation for some modes and the positive-P representation for the remainder. We tested our method on a system of two coupled anharmonic oscillators, one with a mean occupation that remained at 100, the other with a mean occupation of 0.01. The method was able to simulate the evolution of quadrature expectation values for times far beyond where the positive-P method suffers a rapid growth of sampling error. Results were in excellent agreement with the exact solution.

While the truncated Wigner method performed as well as the hybrid method when calculating these quadrature observables (over a finite time), for the calculation of a higher-order

moment corresponding to a QND experiment there was a very clear advantage of the hybrid over the truncated Wigner. The latter results contained large systematic error, while the hybrid result was in excellent agreement with the exact result.

At least as applied to this system with a small number of modes, the hybrid method was able to delay the onset of rapid sampling error growth by a factor of 60 compared to the positive-P method. Further investigations will focus on many-mode systems to see whether these advantages over the earlier methods can be maintained.

It is interesting to note here that our results show that a very natural application of the hybrid method is to systems of two different types of particles with interactions that conserve individual species numbers. This presents a natural framework to investigate quantum Brownian motion, which will be treated in subsequent work.

APPENDIX: EXACT SOLUTIONS

The Hamiltonian

$$\hat{H} = \omega_a \hat{a}^\dagger \hat{a} + \chi_a \hat{a}^\dagger \hat{a}^\dagger \hat{a} \hat{a} + \omega_b \hat{b}^\dagger \hat{b} + \chi_b \hat{b}^\dagger \hat{b}^\dagger \hat{b} \hat{b} + g \hat{a}^\dagger \hat{a} \hat{b}^\dagger \hat{b}, \qquad (A1)$$

describing two coupled anharmonic oscillators, can be written just in terms of the number operators, $\hat{N}_a = \hat{a}^\dagger \hat{a}$ and $\hat{N}_b = \hat{b}^\dagger \hat{b}$, as

$$\hat{H} = \omega_a \hat{N}_a + \omega_b \hat{N}_b + \chi_a (\hat{N}_a^2 - \hat{N}_a) + \chi_b (\hat{N}_b^2 - \hat{N}_b) + g \hat{N}_a \hat{N}_b. \qquad (A2)$$

So the number states

$$|n_a n_b\rangle = \frac{\hat{a}^{\dagger n_a}}{\sqrt{n_a!}} \frac{\hat{a}^{\dagger n_b}}{\sqrt{n_b!}} |0\rangle \qquad (A3)$$

are eigenvectors of the Hamiltonian with eigenvalues

$$E(n_a, n_b) = \omega_a n_a + \omega_b n_b + \chi_a (n_a^2 - n_a) + \chi_b (n_b^2 - n_b) + g n_a n_b. \qquad (A4)$$

We consider an initial state that is a coherent superposition of the number states (A3) of the form

$$|\gamma_a \gamma_b\rangle = \sum_{n_a=1}^{\infty} e^{-1/2|\gamma_a|^2} \frac{\gamma_a^{n_a}}{\sqrt{n_a!}} \sum_{n_b=1}^{\infty} e^{-1/2|\gamma_b|^2} \frac{\gamma_b^{n_b}}{\sqrt{n_b!}} |n_a n_b\rangle, \qquad (A5)$$

where $\gamma_a = \sqrt{N_{a0}}$, $\gamma_b = \sqrt{N_{b0}}$, and N_{a0} and N_{b0} are the average occupations of the modes.

We are interested in observables, Ω, that are simple combinations of a small number of creation and/or annihilation

operators. These have simple matrix elements, $\langle n_a' n_b' | \hat{\Omega} | n_a n_b \rangle$, between the number eigenvectors. All terms will be proportional to Kronecker δ's of the form $\delta_{n_a', n_a + m_a} \delta_{n_b', n_b + m_b}$, for m_a and m_b integers. Then, the expectation value of such an operator in the state vector produced by time evolution of (A5) will always reduce to a double sum (over n_a and n_b), with the unitary time evolution producing a known phase factor inside the sum.

The time-dependent expectation values of the quadrature operators $X_a = \frac{1}{2}(a + a^\dagger)$, $Y_a = \frac{1}{2i}(a - a^\dagger)$, $X_b = \frac{1}{2}(b + b^\dagger)$, and $Y_b = \frac{1}{2i}(b - b^\dagger)$, for the initial state (A5), can then be evaluated as sums over n_a and n_b. We find the results

$$\langle X_a(t) \rangle = \sqrt{N_{a0}} e^{-[N_{a0}(1 - \cos 2\chi_a t) + N_{b0}(1 - \cos gt)]}$$
$$\times \cos\{\omega_a t + N_{a0} \sin 2\chi_a t + N_{b0} \sin gt\}, \quad \text{(A6)}$$

$$\langle Y_a(t) \rangle = -\sqrt{N_{a0}} e^{-[N_{a0}(1 - \cos 2\chi_a t) + N_{b0}(1 - \cos gt)]}$$
$$\times \sin\{\omega_a t + N_{a0} \sin 2\chi_a t + N_{b0} \sin gt\}. \quad \text{(A7)}$$

For $\langle X_b(t) \rangle$ and $\langle Y_b(t) \rangle$, we make the replacement $a \leftrightarrow b$ in expressions (A6) and (A7), respectively.

Our model of a QND measurement has the feature that the coupling strength, g, is constant up to a time, τ, and vanishes after that. This is meant to model two light pulses that cease to interact after they no longer overlap within an optical fiber. The evolution operator for the resulting time-dependent Hamiltonian is $\hat{U}(t) = \exp{-\int_0^t \hat{H}(t') dt'}$. For times up to τ, we evaluate the following:

$$\langle \hat{N}_a \hat{Y}_b(t) \rangle = -N_a \sqrt{N_b} e^{-N_{a0}(1 - \cos gt)} e^{-N_{b0}(1 - \cos 2\chi_b t)} \sin\{(\omega_b + g)t$$
$$+ N_{a0} \sin gt + N_{b0} \sin 2\chi_b t\}, \quad \text{(A8)}$$

$$V(\hat{Y}_b) = \langle \hat{Y}_b^2 \rangle - \langle \hat{Y}_b \rangle^2$$
$$= -\frac{1}{2} N_{b0} e^{-[N_a(1 - \cos 2gt) + N_b(1 - \cos 4\chi_b t)]}$$
$$\times \cos\{2(\omega_b + \chi_b)t + N_a \sin 2gt + N_b \sin 4\chi_b t\}$$
$$- N_b e^{-2[N_a(1 - \cos gt) + N_b(1 - \cos 2\chi_b t)]}$$
$$\times \sin^2\{\omega_b t + N_a \sin gt + N_b \sin 2\chi_b t\} + \frac{1}{4} + \frac{1}{2} N_{b0}. \quad \text{(A9)}$$

For times beyond τ, we make the replacement $gt \to g\tau$ in (A8) and (A9). This rule applies also to the expectation values (A6) and (A7) for $t > \tau$ in this QND scheme.

Finally we note that the individual particle numbers are conserved under this Hamiltonian, and the coherent state initial conditions (A5) give

$$\langle \hat{N}_a \rangle = N_{a0}, \quad \langle \hat{N}_b \rangle = N_{b0}, \quad \text{(A10)}$$

$$V(\hat{N}_a) = N_{a0}, \quad V(\hat{N}_b) = N_{b0}. \quad \text{(A11)}$$

[1] Y. Castin and R. Dum, Phys. Rev. A **57**, 3008 (1998).
[2] N. Bogoliubov, J. Phys. **11**, 23 (1947).
[3] C. W. Gardiner and P. Zoller, Phys. Rev. A **58**, 536 (1998).
[4] B. J. Dalton, J. Phys.: Conf. Ser. **67**, 012059 (2007).
[5] E. P. Wigner, Phys. Rev. **40**, 749 (1932).
[6] J. Moyal, Proc. Cambridge Philos. Soc. **45**, 99 (1949).
[7] A. Gilchrist, C. W. Gardiner, and P. D. Drummond, Phys. Rev. A **55**, 3014 (1997).
[8] C. W. Gardiner and P. Zoller, *Quantum Noise*, 3rd ed. (Springer-Verlag, Berlin, Heidelberg, 2004).
[9] P. Deuar and P. D. Drummond, Phys. Rev. Lett. **98**, 120402 (2007).
[10] L. Plimak *et al.*, Europhys. Lett. **56**, 372 (2001).
[11] K. E. Cahill and R. J. Glauber, Phys. Rev. **177**, 1882 (1969).
[12] J. F. Corney and P. D. Drummond, Phys. Rev. A **68**, 063822 (2003).
[13] R. Graham, *Springer Tracts in Modern Physics* (Springer, New York, 1973), Vol. 66, Chap. 1.
[14] M. J. Steel, M. K. Olsen, L. I. Plimak, P. D. Drummond, S. M. Tan, M. J. Collett, D. F. Walls, and R. Graham, Phys. Rev. A **58**, 4824 (1998).
[15] A. Sinatra, C. Lobo, and Y. Castin, Phys. Rev. Lett. **87**, 210404 (2001).
[16] P. D. Drummond and P. Kinsler, Quantum Semiclassic. Opt. **7**, 727 (1995).
[17] A. J. Leggett, Rev. Mod. Phys. **73**, 307 (2001).
[18] A. A. Norrie, R. J. Ballagh, and C. W. Gardiner, Phys. Rev. Lett. **94**, 040401 (2005).
[19] A. A. Norrie, R. J. Ballagh, and C. W. Gardiner, Phys. Rev. A **73**, 043617 (2006).
[20] R. J. Glauber, Phys. Rev. **131**, 2766 (1963).
[21] E. C. G. Sudarshan, Phys. Rev. Lett. **10**, 277 (1963).
[22] www.xmds.org
[23] P. Deuar and P. D. Drummond, Phys. Rev. A **66**, 033812 (2002).
[24] P. D. Drummond and P. Deuar, J. Opt. B: Quantum Semiclassical Opt. **5**, S281 (2003).
[25] M. R. Dowling, P. D. Drummond, M. J. Davis, and P. Deuar, Phys. Rev. Lett. **94**, 130401 (2005).
[26] S. Chaturvedi and V. Srinivasan, Phys. Rev. A **43**, 4054 (1991).
[27] C. M. Caves *et al.*, Rev. Mod. Phys. **52**, 341 (1980).
[28] M. J. Holland, M. J. Collett, D. F. Walls, and M. D. Levenson, Phys. Rev. A **42**, 2995 (1990).
[29] G. J. Milburn and D. F. Walls, Phys. Rev. A **28**, 2065 (1983).
[30] R. Dong *et al.*, Opt. Lett. **33**, 116 (2008).